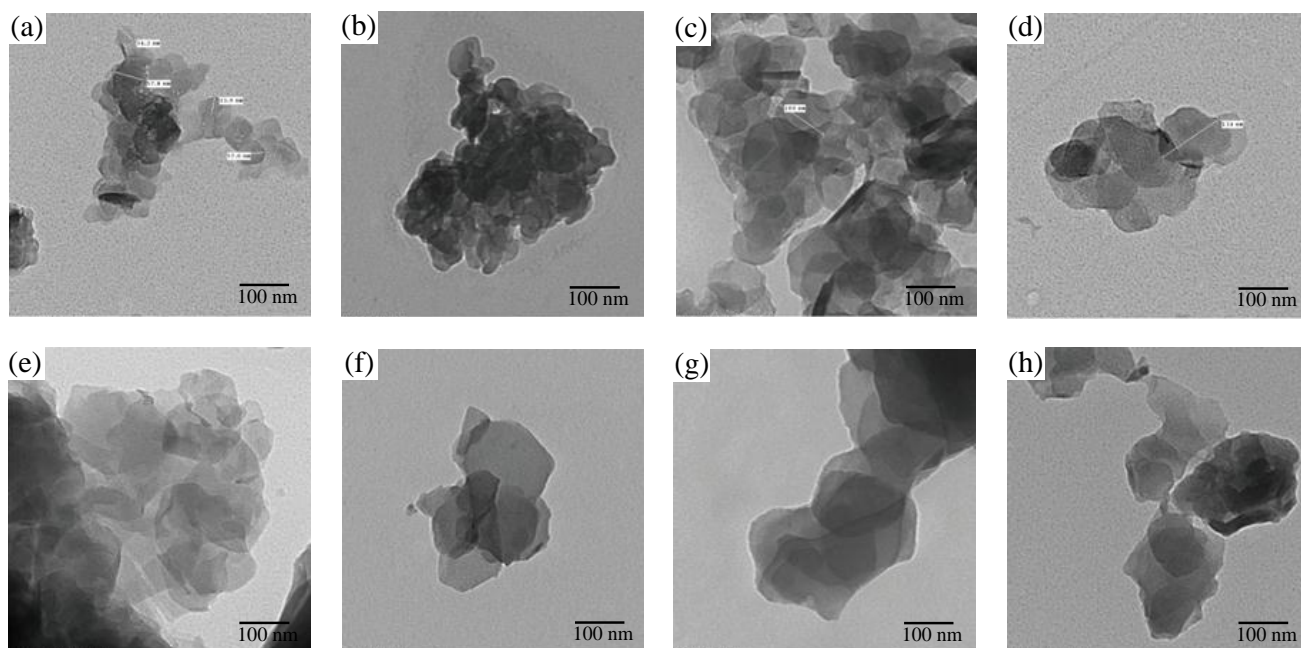
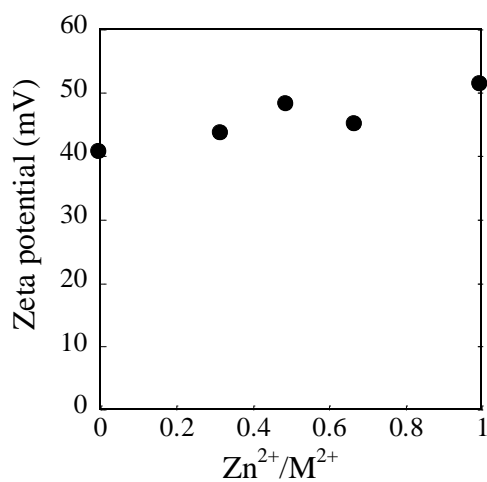


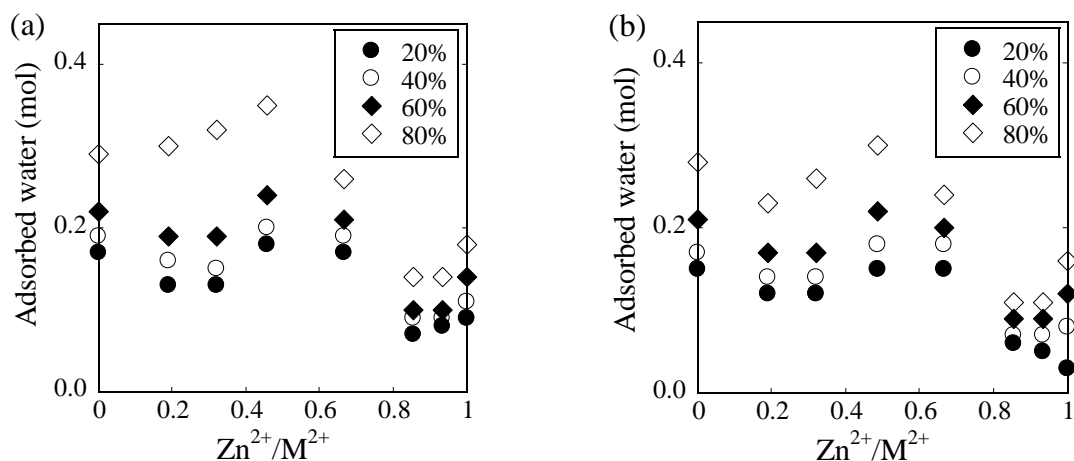
## Supplementary information



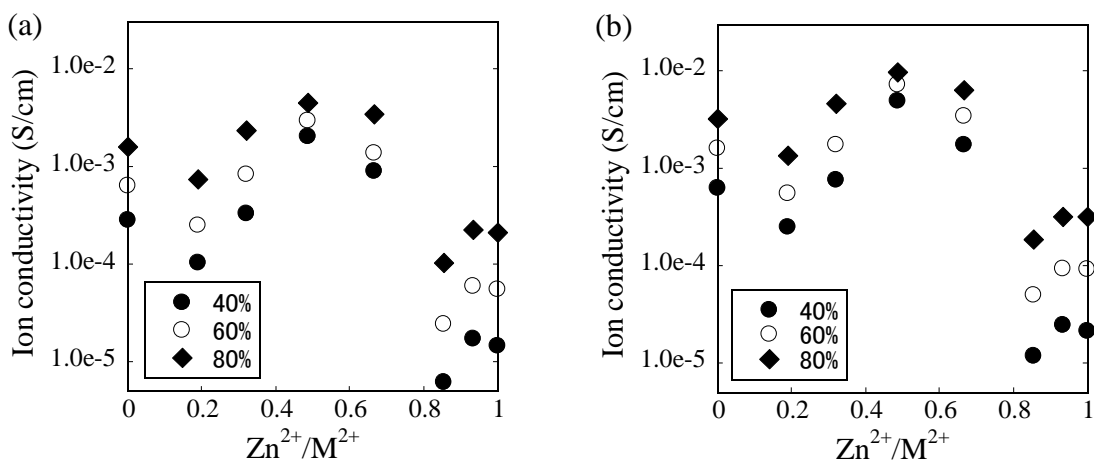
**SI Figure 1.** TEM images of  $(\text{Mg}_{1-x}\text{Zn}_x)_2\text{Al-CO}_3^{2-}$ LDH powder with different  $\text{Zn}^{2+}$ :divalent metals ratios: (a) 0, (b) 0.19, (c) 0.32, (d) 0.49, (e) 0.67, (f) 0.86, (g) 0.94 and (h) 1.00.



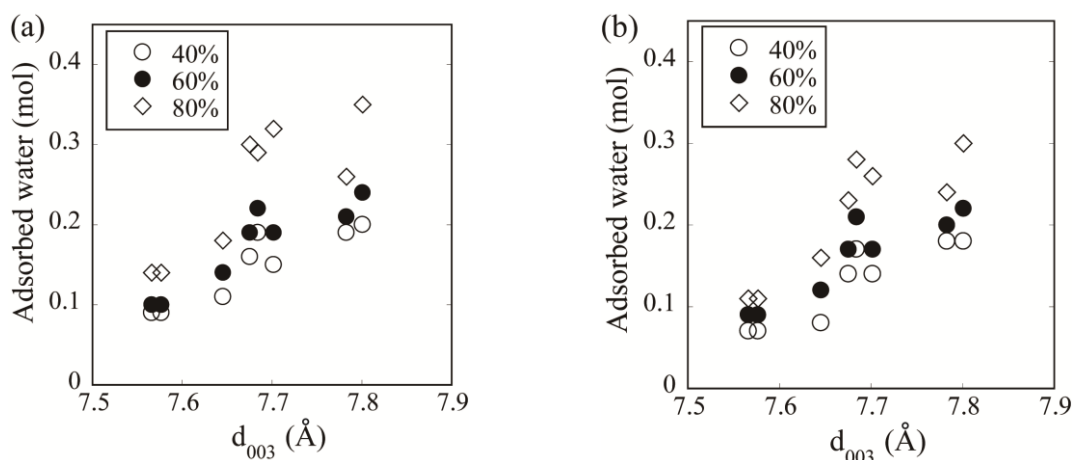
**SI Figure 2.** Plot of zeta potential of  $(\text{Mg}_{1-x}\text{Zn}_x)_2\text{Al-CO}_3^{2-}$ LDHs vs. the  $\text{Zn}^{2+}$ :divalent metals ratio.



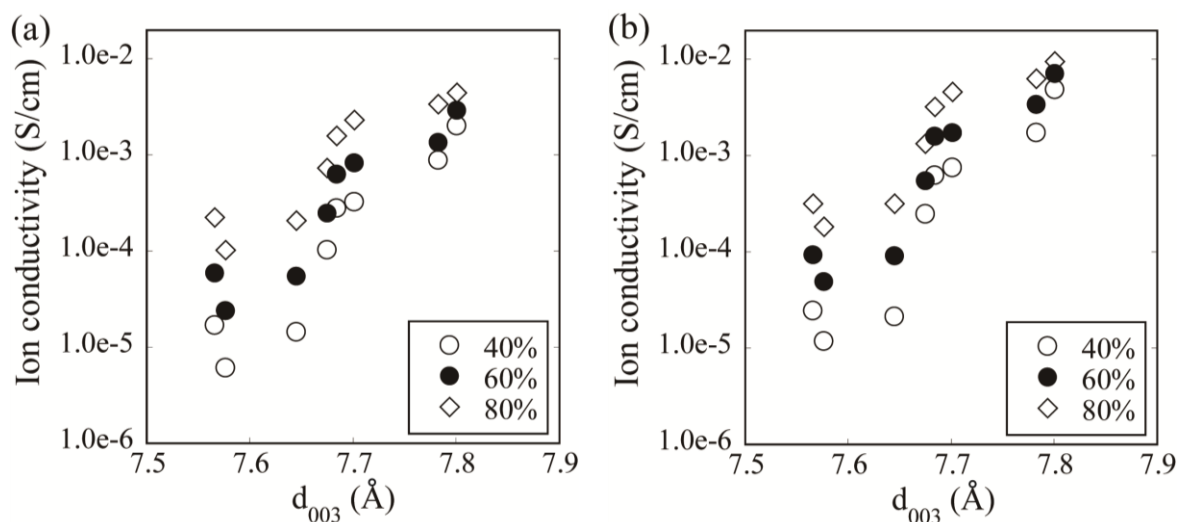
**SI Figure 3.** Amount of adsorbed water per unit molecule,  $[(Mg_{(1-x)}Zn_x)_yAl_z(OH)_2](CO_3^{2-})_{z/2} \cdot nH_2O$  under various humidity conditions at (a) 50 °C and (b) 80 °C, where  $y+z=1$ .



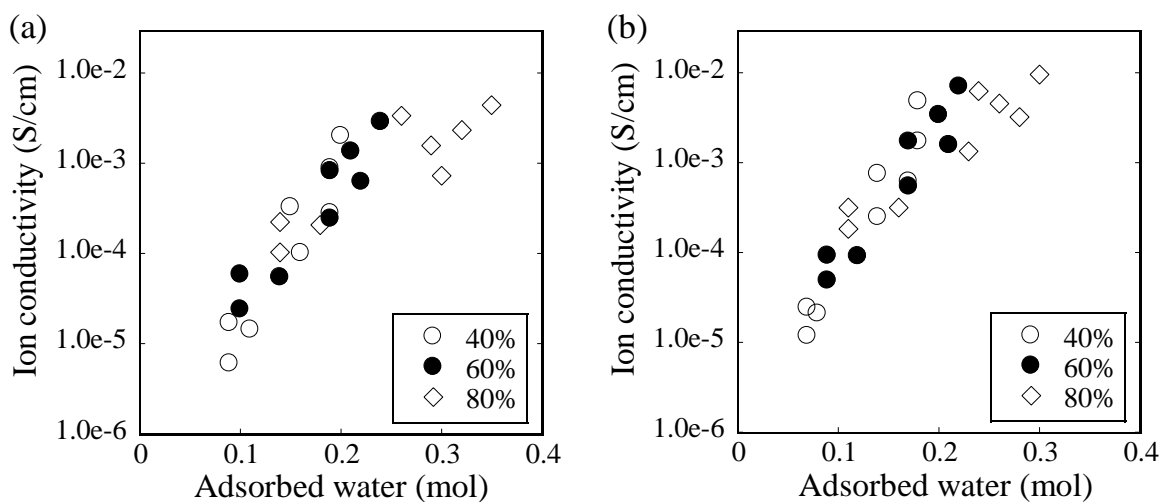
**SI Figure 4.** Ion conductivity of each LDH with different Zn<sup>2+</sup>:divalent metals ratio under various humidity conditions at (a) 50 °C and (b) 80 °C.



**SI Figure 5.** Amount of adsorbed water in unit molecule,  $[(Mg_{(1-x)}Zn_x)_yAl_z(OH)_2](CO_3^{2-})_{z/2} \cdot nH_2O$  at different humidities at (a) 50 °C and (b) 80 °C and interlayer distances ( $d_{003}$ ), where  $y+z=1$ .



**SI Figure 6.** Ion conductivity under various humidity conditions at (a) 50 °C and (b) 80 °C and interlayer distance ( $d_{003}$ ) at room temperature.



**SI Figure 7.** Ion conductivity and adsorbed water under different humidities at (a) 50 °C and (b) 80 °C

**SI Table 1.** Activation energy of ion conduction in  $(\text{Mg}_{(1-x)}\text{Zn}_x)_2\text{Al-CO}_3^{2-}$  LDHs under R.H 80 % from 30 °C to 80 °C, calculated from the Arrhenius plot based on the reference S-1.

$\text{Zn}^{2+}$ :divalent metals ratio (x)	Activation energy (kJ/mol)	$\text{Zn}^{2+}$ :divalent metals ratio (x)	Activation energy (kJ/mol)
0	25	0.67	30
0.19	23	0.86	22
0.32	23	0.94	27
0.49	26	1.00	20

## References

S-1. N. Hara, H. Ohashi, T. Ito and T. Yamaguchi, *J Phys Chem B*, 2009, **113**, 4656-4663.